CHAPTER 5

EXPERIMENTATION ON SHELL-TUBE HEAT EXCHANGER

This chapter presents the development of an experimental setup and the test procedure for the performance investigation of the shell and tube heat exchanger (STHX) using various mono/hybrid nanofluids as a coolant for different operating parameters. In addition, it has data analyses based on energy methodologies. And at last, a detailed explanation of the results obtained in terms of different performance parameters has also been presented.

5.1 Experimental setup and procedure

The layout of the experimental facility, mainly consisting of the shell and tube heat exchanger, temperature-controlled heating tank with immersion heater, cooling unit (chiller) with temperature controller having a cooling capacity of 3 kW, two rotameters, two circulating pumps and U-tube manometer, is shown in Fig. 5.1. In the shell side, the fluids enter at one side and leaves at the other side, i.e., there is one pass on the shell side (E-shell). The E-shell is used because of its simplicity and low cost. Figs. 5.2 (a) and (b) show the photographs of the shell and tube heat exchanger in the horizontal section and a view of tubes inside it. On the tube side, the tubes have two passes and are supported by one baffle. The tube metal is stainless steel (SS 304 Seamless) with external and internal diameters of 19 mm and 15 mm, respectively. Cold fluid (mono/hybrid nanofluid) flows through the tube side and hot fluids (DI water) flows through the shell side in a counter flow direction. The specifications of the shell and tube heat exchanger and operating conditions are summarized in Table 5.1. The asbestos rope was wrapped over the shell side to minimize the heat losses to the environment. The calibrated PT-100 thermometers were used for measuring the temperatures of both fluids. Two rotameters were installed with control valves in each

circular loop to determine the flow rates of the fluids. The control valves were provided to regulate the flow rate. Pressure drops through the inner tube and outer tube were measured by U-tube manometers because of its simplicity and reliability in the operating conditions of the present study. In the experiment, the inlet temperature of cold fluid was kept at 30^{o}C and the flow rate was varying from 6 to10 lpm. The hot fluid was maintained at a constant temperature of 60^{o}C with a constant flow rate of 25 lpm. In each test run, all the temperatures, as well as pressure drops, were recorded after reaching the steady-state.

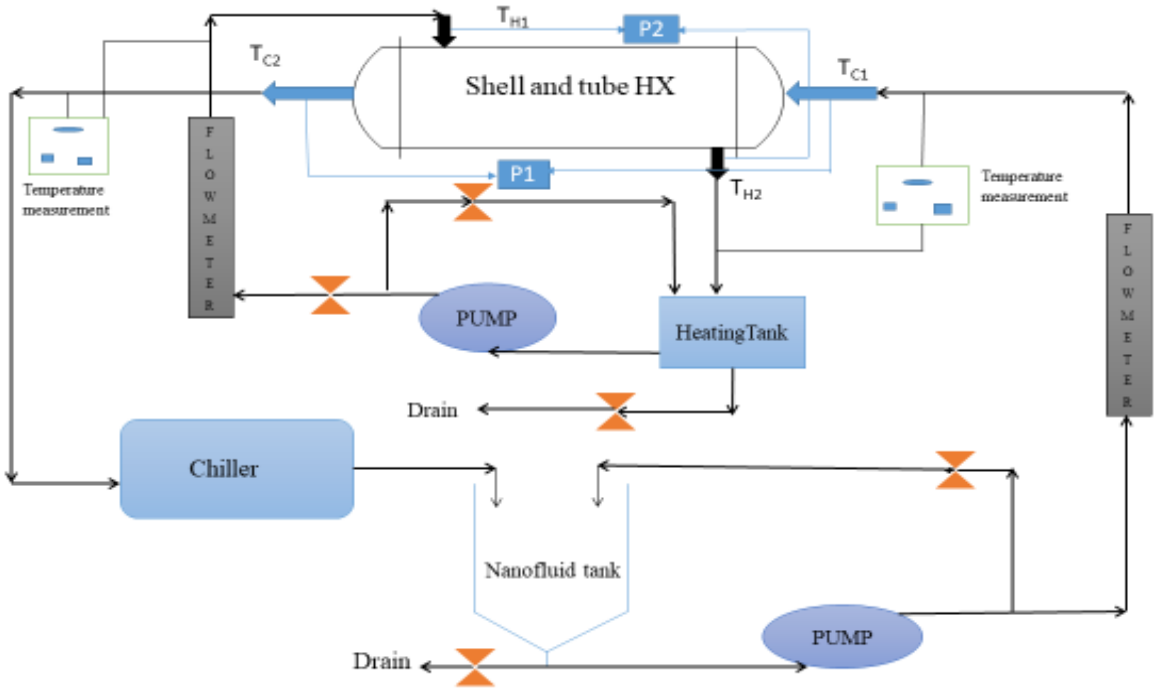

Figure 5.1. Schematic diagram of the experimental setup (STHX)

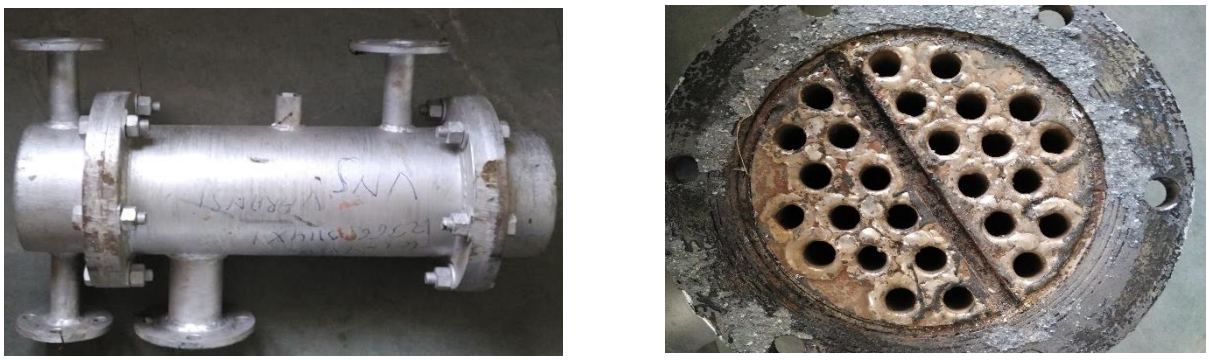

(a) (b)

Figure 5.2. Photographs of shell-and-tube heat exchanger (a) Horizontal section (b) tubes

Table 5.1- Details of the experimental setup and operating condition

Parameters	Value
Shell Diameter	150 mm
Shell Thickness	7 to 8 mm
Overall Length of Equipment	600 mm
Shell Material	MS Seamless
Tube Size	(19mm OD, 15 mm ID) (SS 304 Seamless)
No. of Tubes	26
No. of Baffles	1
Reynolds number, (Re)	900 to 1500
Flow in tube and shell side	Laminar and Turbulent
Cold nanofluid inlet temperature	30^{o}C
Hot fluid inlet temperature	60^{o}C

5.2 Data reduction

Hybrid nanofluid heat transfer rate in tube side is given by the equation

$$q_{nf} = \dot{V}_{nf}\ \rho_{nf}.c_{pnf}.(T_{nf,out} - T_{nf,in}) \tag{5.1}$$

For PCM dispersed mono/hybrid nanofluid, the heat transfer rate is calculated by,

$$q_{nf} = \dot{V}_{nf}\ \rho_{nf} c_{pnf}\left(T_{nf,out} - T_{nf,in}\right) + \varphi_{PCM}\,\dot{V}\,\rho_{PCM,solid} L_{PCM} \tag{5.2}$$

The mean velocity of mono/hybrid nanofluid is calculated using,

$$\dot{V}_{nf} = u_m.\frac{\pi}{4}.d_i^{\,2}.N_t \tag{5.3}$$

Where N_t and d_i are the number of tubes and the inside diameter of the tube, respectively.

The tube side Reynolds number is given by,

$$\mathrm{Re}_{nf} = \frac{\rho_{nf}.u_m.d_i}{\mu_{nf}} \tag{5.4}$$

The Prandtl number is given by

$$\mathrm{Pr}_{nf} = \frac{c_{pnf}.\mu_{nf}}{k_{nf}} \tag{5.5}$$

Hot fluid (DI water) heat transfer rate in shell side is calculated by,

$$q_h = \dot{V}_h \rho_h c_{ph} \left(T_{h,in} - T_{h,out}\right) \tag{5.6}$$

Instead of insulation, there is some difference in the value of q_{nf} and q_h. To ensure the accuracy of the results, the average heat transfer rate is taken, which is determined by,

$$q_{avg} = \left(q_{nf} + q_h\right)/2 \tag{5.7}$$

Overall heat transfer coefficient for tube side,

$$U_i = \frac{q_{avg}}{A_i \times \Delta T_{LMTD}} \tag{5.8}$$

Where,

$$\Delta T_{LMTD} = \frac{\left(T_{h,in} - T_{nf,out}\right) - \left(T_{h,out} - T_{nf,in}\right)}{\ln\left(\frac{T_{h,in} - T_{nf,out}}{T_{h,out} - T_{nf,in}}\right)} \tag{5.9}$$

The tube side heat transfer coefficient (h_i) is calculated by the equation without considering fouling

$$\frac{1}{U_i A_i} = \frac{1}{h_i A_i} + \frac{\ln\left(\frac{d_o}{d_i}\right)}{2\pi kL} + \frac{1}{h_o A_o} \tag{5.10}$$

Where, h_o, k and L represents the shell side heat transfer coefficient, thermal conductivity of the tube material and length of the tube, respectively.

Nusselt number of shell side is calculated by using correlation developed by McAdams **(Kakac and Liu, 2002),**

$$Nu_o = 0.36\,\mathrm{Re}_s^{0.55}\,\mathrm{Pr}^{1/3}\left(\frac{\mu}{\mu_w}\right)^{0.14} \tag{5.11}$$

Range: 2000 < Re_s < 10^6

The shell side heat transfer coefficient can be calculated as:

$$h_o = \frac{Nu_o \times k_o}{d_{eqv}} \tag{5.12}$$

Where d_{eqv} is equivalent diameter and k_o is the thermal conductivity of the shell side fluid

$$d_{eqv} = \frac{4\left\{\frac{\sqrt{3}P_T^{\,2}}{4} - \frac{\pi d_o^{\,2}}{8}\right\}}{\pi d_o / 2} \tag{5.13}$$

Where d_o is the tube outside diameter

The Nusselt number of hybrid nanofluid can be determined by the equation;

$$Nu_{nf} = \frac{h_{nf} \times d_i}{k_{nf}} \tag{5.14}$$

The pressure drop in the tube is calculated by the following equation,

$$\Delta p = \Delta p_{\exp} - \rho g(Loss_{head}) \tag{5.15}$$

The combined header and tube entrance losses are estimated by,

$$Loss_{head} = \gamma \frac{u_m^{\,2}}{2g} \tag{5.16}$$

where γ is pressure loss coefficient

The friction factor is estimated based on pressure difference and expression is given below;

$$f = \frac{\pi^2}{8}\Delta p\left(\frac{\rho_{nf} d_{it,i}^{\,5}}{\dot{m}_{nf}^{\,2} L}\right) \tag{5.17}$$

5.3. Results and discussion

5.3.1 Validation with DI water

The experimental setup is validated by conducting the experiments with DI water where cold fluids flowing in the tube side and hot fluid flowing in the shell side. Parameters such as temperatures and pressure drop were recorded at the range of Reynolds number from 900-1600 after reaching steady-state for determining the Nusselt number and friction factor. The experimental Nusselt number and friction factor are measured using the equation (5.14) and (5.17). The experimental results of the Nusselt number are compared with Seider and Tate correlation **(Incopera et al., 2006)** and the results of the friction factor are compared with the Darcy Weisbach equation for laminar flow **(Incopera et al., 2006)**. Figs. 5.3 (a) and (b) show the comparison of correlation with experimental data of Nusselt number and friction factor, respectively. It was observed that the experimental data were in good agreement with the correlation and exhibited an average deviation of 8.24 % in the Nusselt number and 8.38% in friction factor.

Seider and Tate correlation for laminar flow

$$Nu = 1.86\left(\mathrm{Re}\,\mathrm{Pr}\frac{D}{L}\right)^{1/3}\left(\frac{\mu_b}{\mu_w}\right)^{0.14} \tag{5.18}$$

Darcy Weisbach equation for laminar flow

$$f = \frac{64}{\mathrm{Re}} \tag{5.19}$$

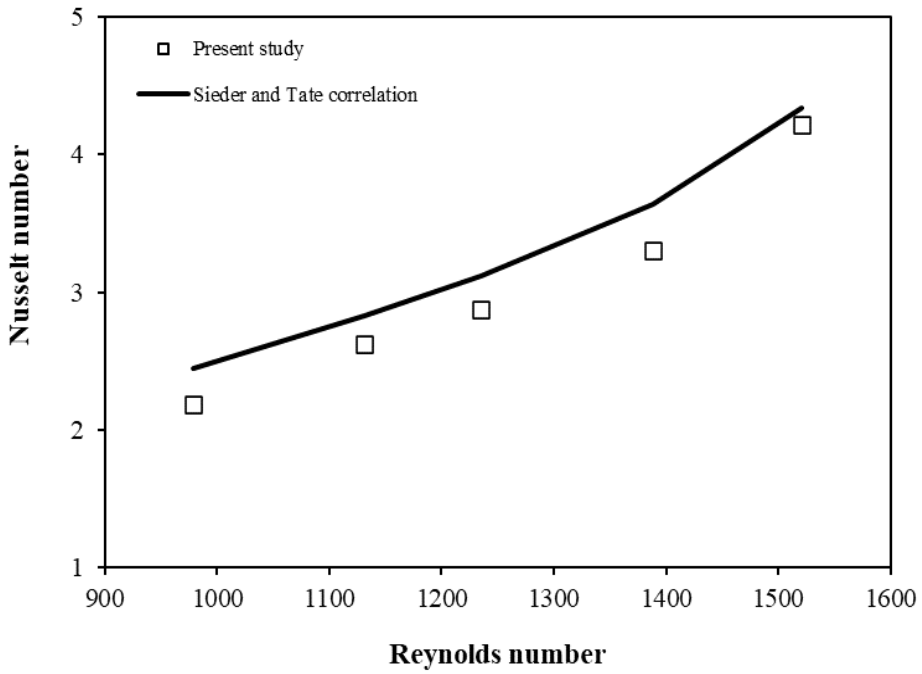

(a) Nusselt number

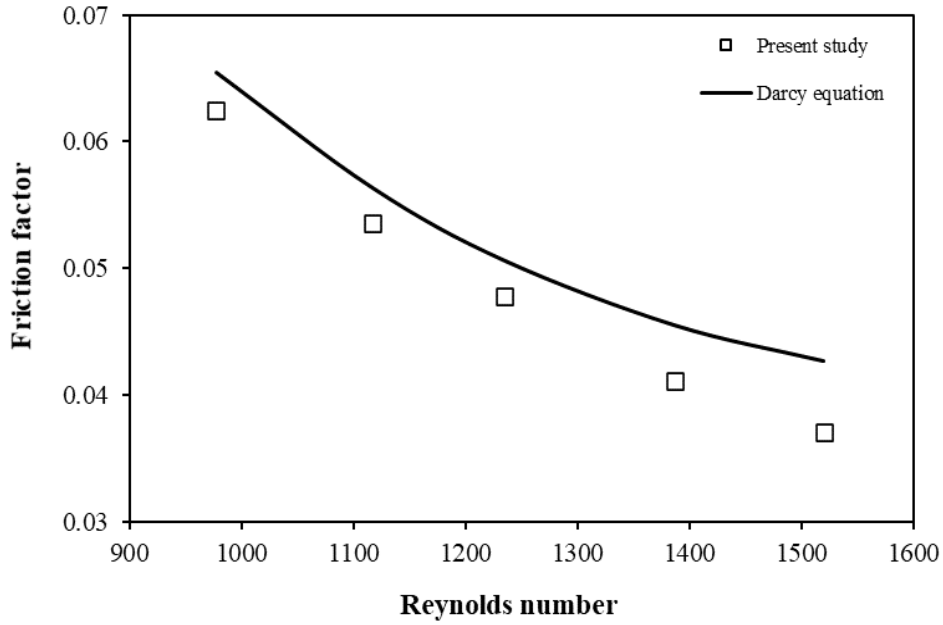

(b) Friction factor

Figure 5.3 (a) and (b) Validation with DI water

5.3.2 Comparison of different hybrid nanofluids

Figs. 5.4 and 5.5 show the influence of different hybrid nanofluids with the same volume concentration (0.01% vol.) on the heat transfer coefficient (h_i) and pressure drop (Δp) with the variation of volume flow rate. The results indicate that h_i and Δp considerably increase with the increase in the nanofluid flow rate because when the volume flow rate increases, it affects the increasing intensity of turbulence in the flow. In addition, both are higher than those of DI water. With the addition of nanoparticles in the base fluid, it increases the thermal conductivity and fluid viscosity, which are the key factors for the enhancement of the heat transfer and pressure drop. The maximum value of h_i is observed for Al_2O_3+CNT hybrid nanofluid, i.e., 231.71 W/m^{2}K followed by CNT (221.84 W/m^{2}K), Al_2O_3+PCM (193.80 W/m^{2}K), PCM (185.93 W/m^{2}K) and Al_2O_3 (185.82 W/m^{2}K) hybrid nanofluid and the maximum value of Δp is observed 533.66 Pa for Al_2O_3+CNT followed by CNT (515.15 Pa), PCM (500.31Pa), Al_2O_3+PCM (490.30 Pa) and Al_2O_3 (480.29 Pa) hybrid nanofluid respectively, at a higher flow rate (10 lpm). At the high flow rate (10 lpm), Al_2O_3+CNT enhances around 37.85% in the heat transfer coefficient and 14.28% in pressure drop as compared to that of DI water. CNT dispersed mono/hybrid nanofluids exhibit a higher heat transfer coefficient due to higher thermal conductivity and also higher pressure drop due to high viscosity. Also, the results reveal that in the case of PCM dispersed mono/hybrid nanofluids, PCM shows a higher heat transfer coefficient at a low flow rate. The coolants have a longer time to absorb heat from the hot fluids at a low flow rate and increase the phase change processes completely, which increases the heat transfer of the coolant and energy storage in PCM particles as the latent heat. At a higher flow rate, PCM shows a higher pressure drop due to the increased dynamic viscosity by the addition of phase change particles.

Fig. 5.6 shows the variation of the ratio $h_i/\Delta p$ with respect to the nanofluid flow rate. As seen in Fig 5.6, the ratio $h_i/\Delta p$ decreases with an increase in the nanofluid flow rate for all cases of working fluids. The ratio $h_i/\Delta p$ yields maximum value at a low flow rate as h_i dominances over Δp at a low flow rate. Among all working fluids, PCM shows maximum $h_i/\Delta p$ value at a low flow rate of 6 lpm. It is also observed that at the low flow rate, Al_2O_3, Al_2O_3+PCM, CNT and Al_2O_3+CNT of 0.01 vol.% concentration nanofluid have lower $h_i/\Delta p$ value than DI water irrespective of the increase in heat transfer coefficient, due to the fact that the pressure drop increment dominants over the heat transfer coefficient at a low flow rate.

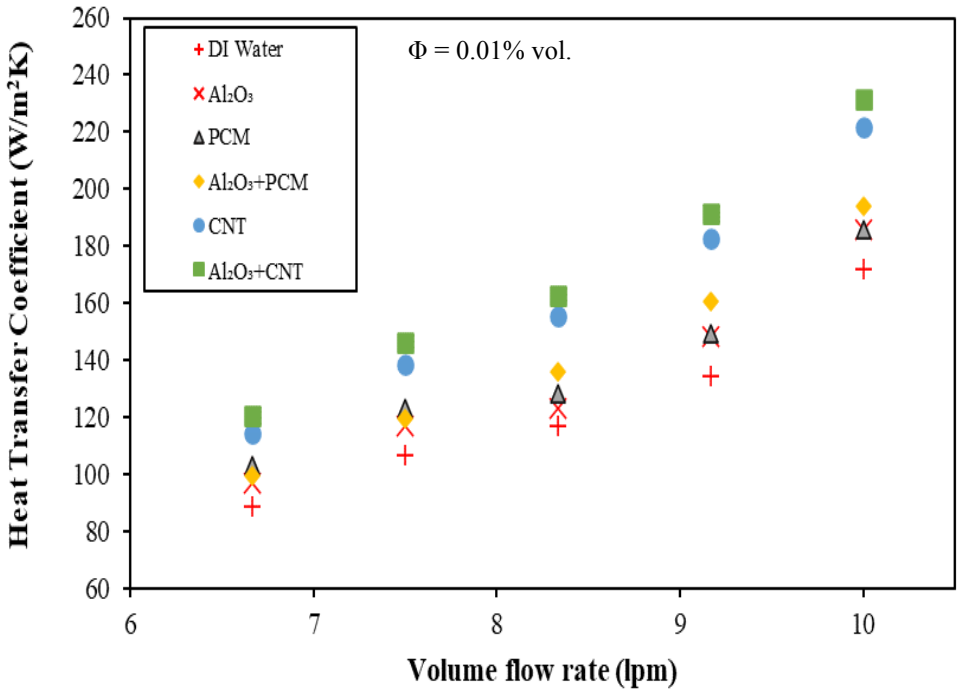

Figure 5.4. Heat transfer coefficient versus nanofluid flow rate for different nanofluids

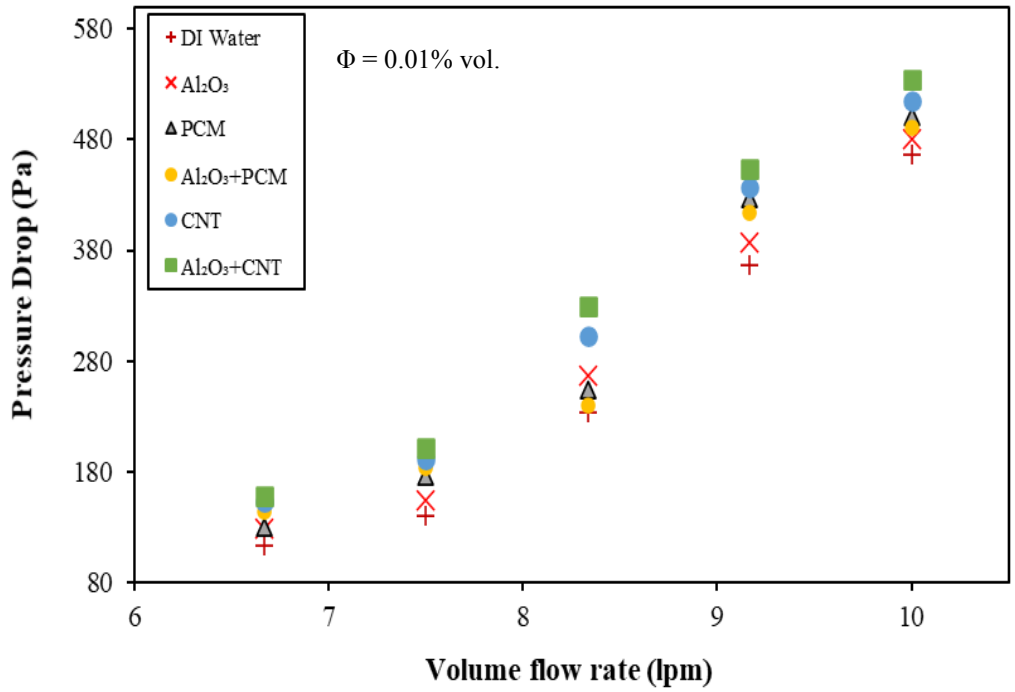

Figure 5.5. Pressure drop versus nanofluid flow rate for different mono and hybrid nanofluid

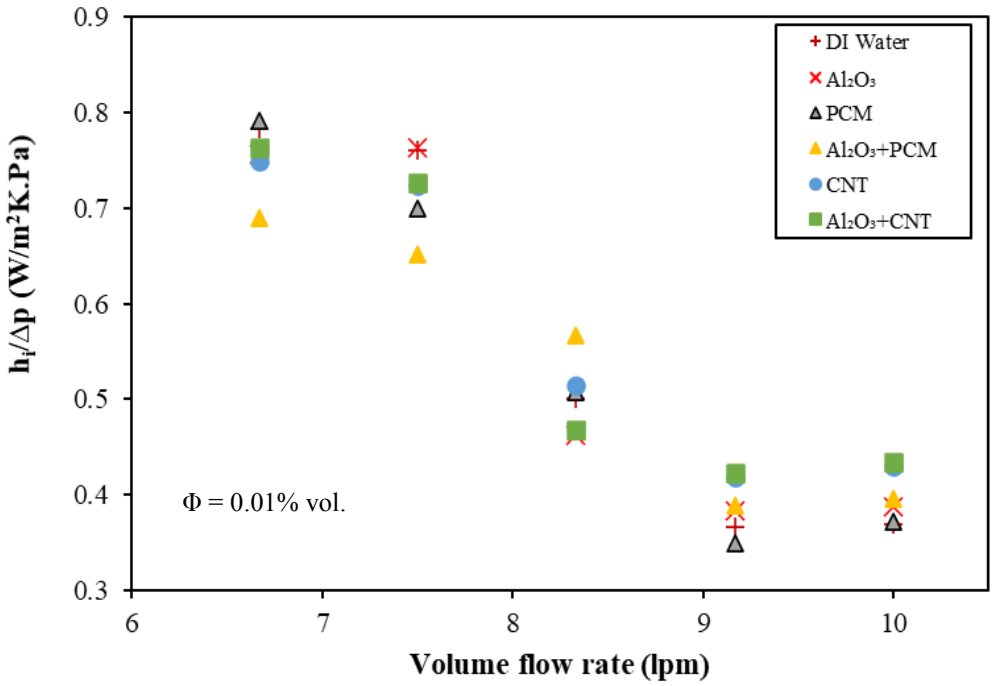

Figure 5.6. Variation of ratio $h_i/\Delta p$ with flow rate for different mono/hybrid nanofluids

The variations of Nusselt number and friction factor with Reynolds number for different mono/hybrid nanofluids at the same volume concentration of 0.01% are illustrated in Figs. 5.7 and 5.8. The results show that the Nusselt number increases and the friction factor decreases with increasing Reynolds number. Both the Nusselt number and friction factor of mono/hybrid nanofluids are greater than that of the base fluid (water). It is due to the increase of thermal conductivity of nanoparticles and the increase of fluid viscosity, which causes to be lost of fluid movement, which promotes better heat transfer. The maximum value of Nusselt number is observed for Al_2O_3+CNT hybrid nanofluid (i.e., 5.68), followed by CNT (5.44), Al_2O_3+PCM (4.75), PCM (4.56) and Al_2O_3 (4.55) hybrid nanofluid, respectively, at high Reynolds number (Re =1500). The average Nusselt number and friction factor of Al_2O_3+CNT hybrid nanofluid flowing in the tube enhance by 38.08% and 15.60%, respectively, as compared to DI water (base fluid) at the Reynolds number of 1500. In the case of PCM dispersed mono/hybrid nanofluids, PCM nanofluid shows higher Nusselt number and friction factor at low Reynolds number while Al_2O_3+PCM hybrid nanofluid shows higher at high Reynolds number.

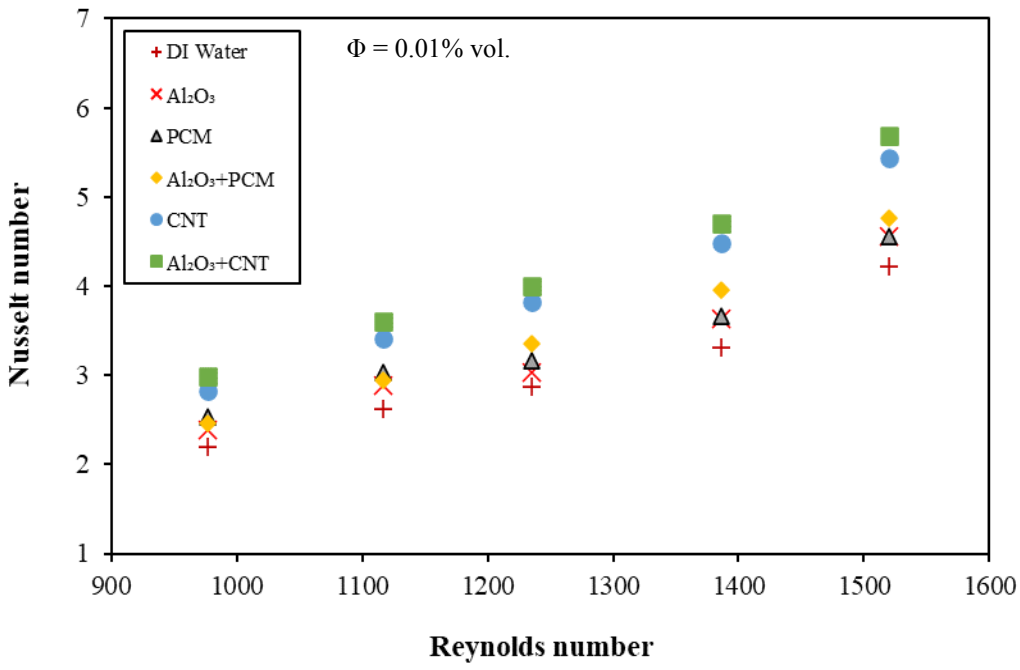

Figure 5.7. Nusselt number versus Reynolds number for different mono and hybrid nanofluid

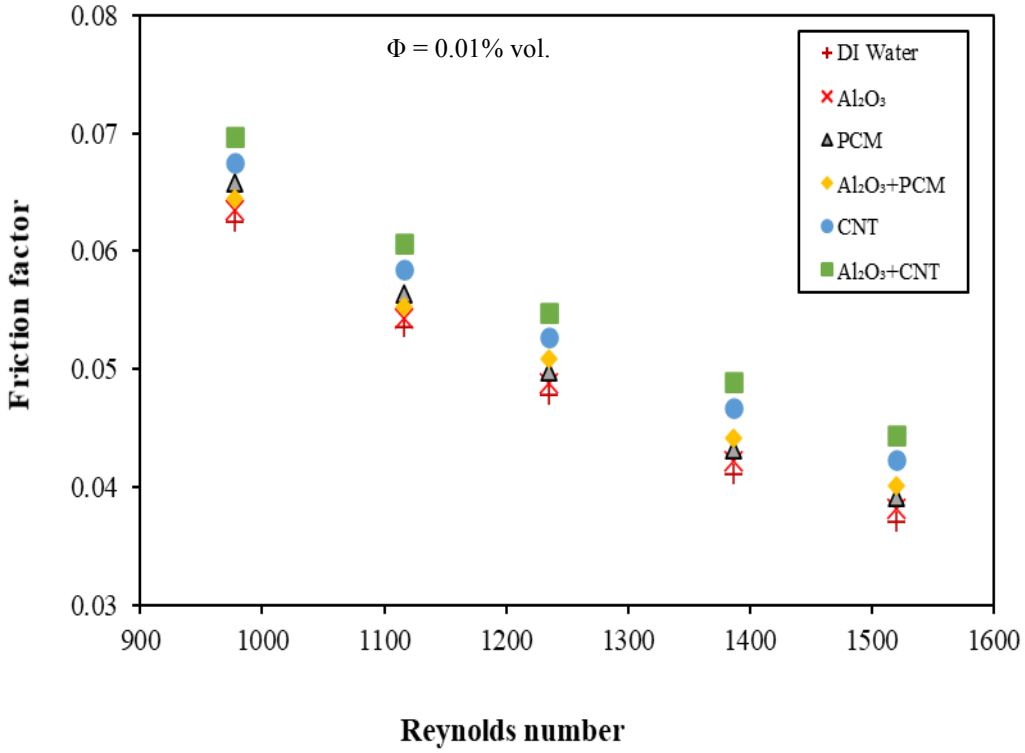

Figure 5.8. Friction factor versus Reynolds number for different mono and hybrid nanofluid

5.3.3 Effects of particle volume concentration

The variations of heat transfer coefficient and pressure drop of different mono and hybrid nanofluids (Al_2O_3, PCM and Al_2O_3+PCM) for different particle volume concentrations (0.01%-0.1% vol.) at a volume flow rate of 8.33 lpm are illustrated in Figs. 5.9 and 5.10. The results indicate that h_i and Δp increase with an increase in particle volume concentration. Also, the results reveal that Al_2O_3+PCM hybrid nanofluid shows insignificantly higher heat transfer coefficient as compared to that of PCM and Al_2O_3 nanofluids for different volume concentrations. PCM nanofluid shows a higher pressure drop, followed by Al_2O_3+PCM hybrid nanofluid and Al_2O_3 nanofluid. The heat transfer coefficient and pressure drop increase with an increase in volume concentration because of the enhancement in thermo-physical properties of the hybrid nanofluid, such as viscosity, density and thermal conductivity. When the volume concentration increases from 0.01 to 0.1%, the

augmentation of 9.18% in the heat transfer coefficient for Al_2O_3+PCM hybrid nanofluid and 36.84% in pressure drop for PCM nanofluid were found at a flow rate of 8.33 lpm.

Fig. 5.11 illustrates the variations of the ratio $h_i/\Delta p$ of different mono and hybrid nanofluids (Al_2O_3, PCM and Al_2O_3+PCM) for different volume concentrations (0.01%-0.1% vol.) at a volume flow rate of 8.33 lpm. The result reveals that while increasing particle volume concentration from 0.01-0.1%, the $h_i/\Delta p$ value increases for Al_2O_3 as the heat transfer coefficient dominances over the pressure drop and the $h_i/\Delta p$ value decreases for PCM and Al_2O_3+PCM nanofluids as pressure drop increment dominants over the heat transfer coefficient. Among all working fluids, Al_2O_3+PCM of 0.01 vol. % concentration shows the maximum value of the ratio $h_i/\Delta p$, i.e., 0.57.

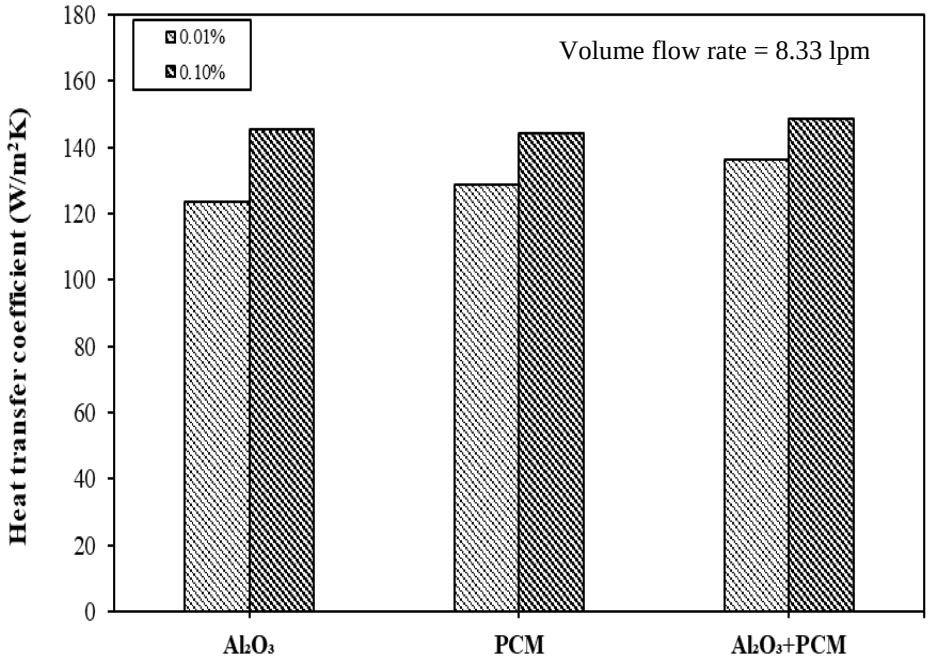

Figure 5.9. Variation of heat transfer coefficient with different particle volume concentration

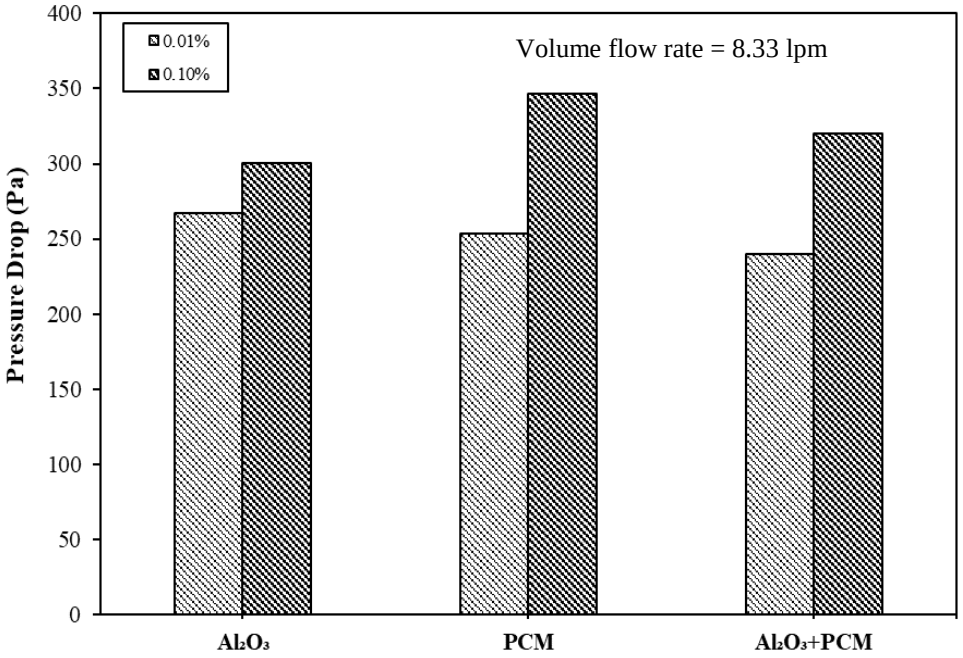

Figure 5.10. Variation of pressure drop with different particle volume concentration

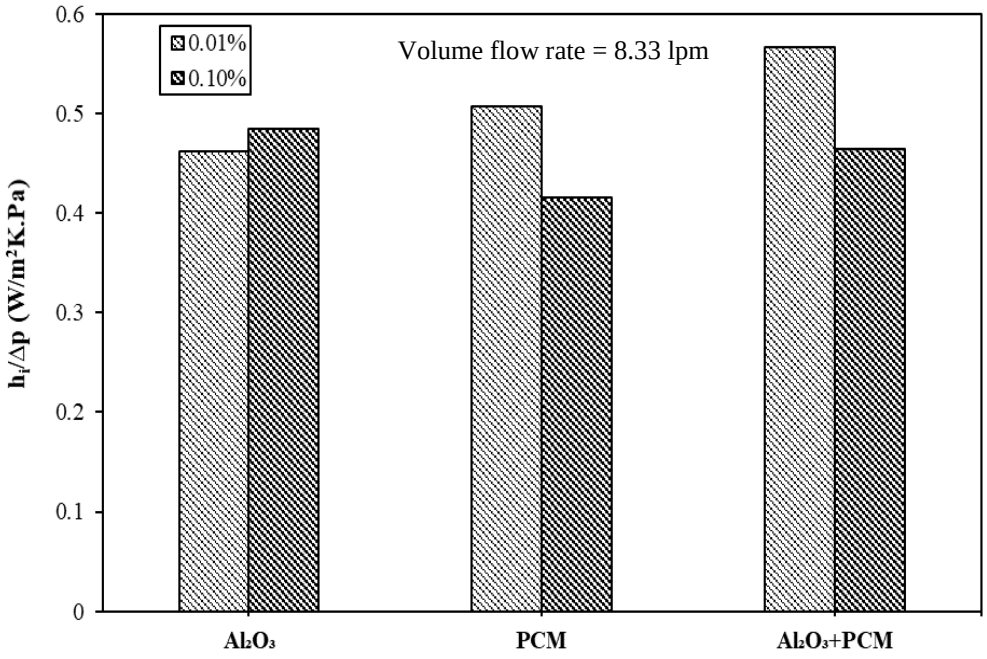

Figure 5.11. Variation of ratio $h_i/\Delta p$ with different particle volume concentration

Figs. 5.12 and 5.13 show the variations of Nusselt number and friction factor of different particle volume concentrations (0.01%-0.1% vol.) for different mono and hybrid nanofluid (Al_2O_3, PCM and Al_2O_3+PCM) at a flow rate of 8.33 lpm. The results reveal that

the Nusselt number and friction factor considerably increase with an increase in particle volume concentration. Also, the results reveal that Al_2O_3+PCM hybrid nanofluid shows a higher Nusselt number and friction factor as compared to that of PCM and Al_2O_3 nanofluid for different volume concentrations due to the dual effect of increasing heat capacity and thermal conductivity. The Nusselt number and friction factor increases because of the enhancement in thermo-physical properties of the hybrid nanofluid, such as viscosity, density and thermal conductivity. When the volume concentration increases from 0.01 to 0.1%, the augmentation of 8.91% in the Nusselt number and 5.98% in friction factor for Al_2O_3+PCM was found respectively at a flow rate of 8.33 lpm.

Fig 5.14 shows the variation of the effectiveness with Reynolds number for different mono/hybrid nanofluids of 0.01% volume concentration. The result reveals that the effectiveness of the shell and tube heat exchanger using mono/hybrid nanofluids is higher than that of the DI water. Among all working fluids, Al_2O_3+CNT hybrid nanofluid shows a higher value of effectiveness. The maximum effectiveness was obtained, i.e., 0.164 at the Reynolds number of 1520. Nanofluid with higher thermal conductivity exhibits better heat transfer, which leads to an increase in the temperature difference, which in turn increases the effectiveness. As compared to DI water, the effectiveness of the shell and tube heat exchanger enhances around 28.65 % using Al_2O_3+CNT hybrid nanofluid.

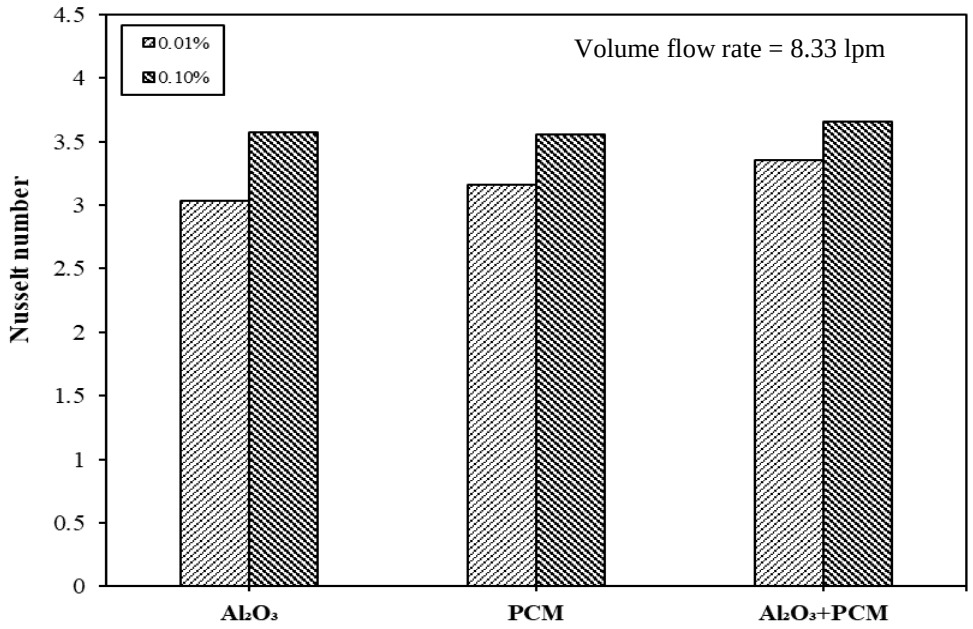

Figure 5.12. Variation of Nusselt number with different particle volume concentration

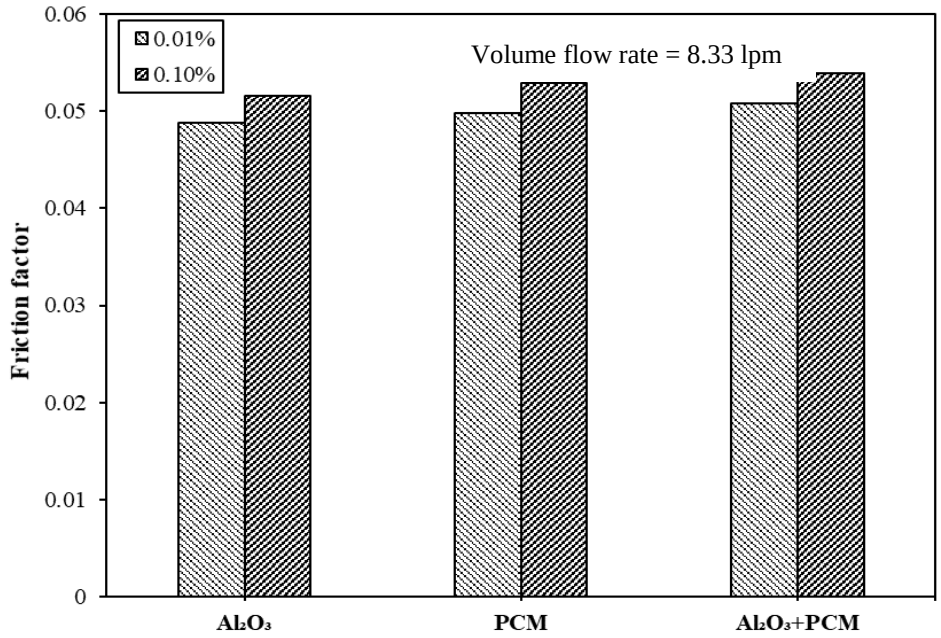

Figure 5.13. Variation of friction factor with different particle volume concentration

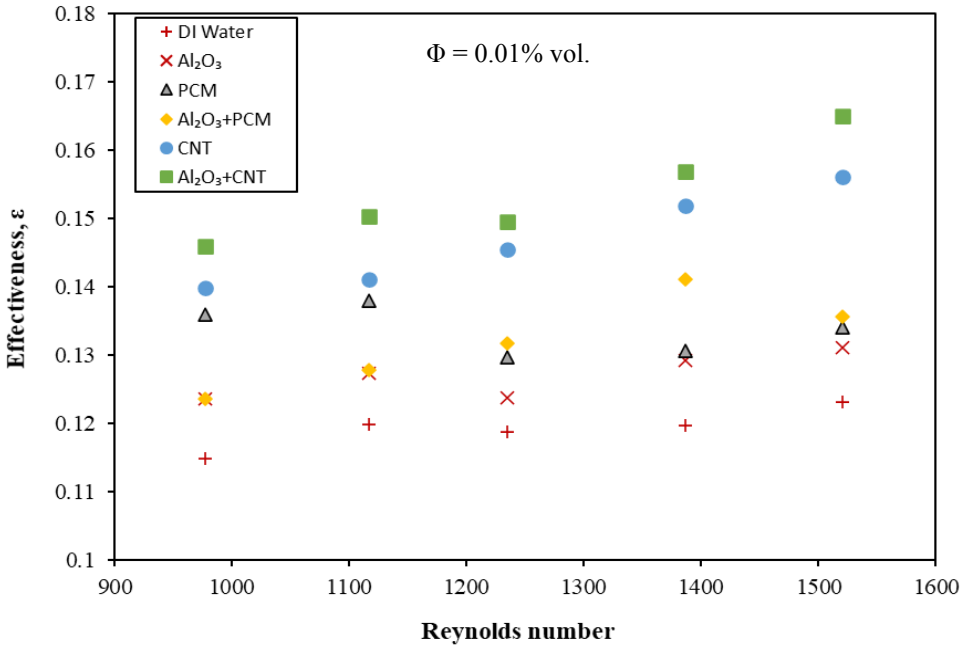

Figure 5.14. Variation of effectiveness with different mono/hybrid nanofluids

5.4 Highlights

Experimental analyses for hydrothermal performance in shell and tube heat exchanger using different nanofluids (Al_2O_3, PCM, CNT, Al_2O_3+PCM and Al_2O_3+CNT) at volume concentrations of 0.01% and 0.1% were conducted under laminar flow condition. Following conclusions can be drawn:

- The heat transfer coefficient and pressure drop considerably increase with the nanofluid flow rate. In addition, both are higher than those of DI water and enhance with volume concentration.
- The maximum value of heat transfer coefficient is observed for Al_2O_3+CNT hybrid nanofluid, i.e., 231.71 W/m^{2}K followed by CNT (221.84 W/m^{2}K), Al_2O_3+PCM (193.80 W/m^{2}K), PCM (185.93 W/m^{2}K) and Al_2O_3 (185.82 W/m^{2}K) hybrid nanofluid and the higher value of pressure drop is found 533.66 Pa for Al_2O_3+CNT followed by CNT (515.15 Pa), PCM (500.31Pa), Al_2O_3+PCM (490.30 Pa) and Al_2O_3 (480.29 Pa) hybrid nanofluid respectively, at a higher flow rate (10 lpm)

- The ratio $h_i/\Delta p$ decreases with an increase in the nanofluid flow rate for all cases of working fluids. While increasing particle volume concentration from 0.01-0.1%, the $h_i/\Delta p$ value increases for Al_2O_3 as the heat transfer coefficient dominates over the pressure drop and the $h_i/\Delta p$ value decreases for PCM and Al_2O_3+PCM nanofluids as pressure drop increment dominants over the heat transfer coefficient.
- The Nusselt number increases and the friction factor decreases with increasing the Reynolds number. The average Nusselt number and friction factor of Al_2O_3+CNT hybrid nanofluid flowing in the tube enhance by 38.08% and 15.60%, respectively, as compared to the base fluid at the volume flow rate of 10 lpm.
- In the case of PCM dispersed mono/hybrid nanofluids, PCM shows a higher heat transfer coefficient at a low flow rate. At a higher flow rate, PCM shows a higher pressure drop due to the increased dynamic viscosity by the addition of phase change particles.
- When the volume concentration increases from 0.01 to 0.1%, the augmentation of 9.18% in the heat transfer coefficient, 8.91% in the Nusselt number and 5.98% in friction factor for Al_2O_3+PCM and 36.84% in pressure drop for PCM was found respectively at a flow rate of 8.33 lpm.
- Among all working fluids, Al_2O_3+CNT hybrid nanofluid shows a higher value of effectiveness. The maximum effectiveness was obtained, i.e., 0.164 at the Reynolds number of 1520.